

Catalysis Science & Technology

Tuneable, In Situ-Generated Nickel-Hydride Alkene Isomerisation Catalyst

Journal:	Catalysis Science & Technology
Manuscript ID	CY-ART-08-2024-000974.R1
Article Type:	Paper
Date Submitted by the Author:	19-Sep-2024
Complete List of Authors:	Kascoutas, Melanie; University of Oregon, Chemistry and Biochemistry Chang, Alison; University of Oregon, Chemistry and Biochemistry Kawamura, Kiana; University of Oregon, Chemistry and Biochemistry Bailey, Gabriela; University of Oregon, Chemistry and Biochemistry Morris, Parker; University of Oregon, Chemistry and Biochemistry Borst, Elizabeth; University of Oregon, Chemistry and Biochemistry Granados, Lilliana; University of Oregon, Chemistry and Biochemistry Cook, Amanda; University of Oregon, Chemistry and Biochemistry

SCHOLARONE™ Manuscripts

ARTICLE

Tuneable, *In Situ*-Generated Nickel-Hydride Alkene Isomerisation Catalyst[†]

Received 00th January 20xx, Accepted 00th January 20xx

DOI: 10.1039/x0xx000000x

Melanie A. Kascoutas, a Alison Sy-min Chang, Kiana E. Kawamura, Gabriela M. Bailey, Parker T. Morris, Elizabeth A. Borst, Lilliana H. Granados, Amanda K. Cook*,

A modular, operationally practical Ni(0)/silane alkene isomerisation system has been developed with air-tolerant reagents. An attractive feature of this method is the ability to rapidly screen a variety of N-heterocyclic carbene (NHC) ligands, enabling optimization through ancillary ligand backbone modification for enhanced reactivity. This system is is readily scalable (>1 g alkene) and tolerates a diverse array of functional groups in high E-selectivity, including aryl bromides, heterocycles, tertiary amines, and α,β -unsaturated amides. Preliminary mechanistic experiments support a Ni–H insertion/elimination pathway.

Introduction

Alkenes are abundant feedstock chemicals frequently used in a variety of synthetic applications like constructing natural products, pharmaceuticals, and commodity chemicals.^{1,2} One efficient route to synthesize internal alkenes is through transition metal-catalysed alkene isomerisation, which typically converts terminal alkenes to form the thermodynamically stable product (Fig. 1a).2 Alkene isomerisation is invoked in important processes such as the DuPont adiponitrile process; in this process, a homogeneous Ni-H active catalyst, is used to contra-thermodynamically migrate an alkene from an internal to a terminal position before hydrocyanation (Fig. 1b).1 Alkene isomerisation catalysts composed of 2nd and 3rd row transition metals have been designed to control specific positional and geometric (E/Z) selectivities; however, recent focus has shifted to the development of Earth-abundant base metals as more sustainable and economical alternatives to precious-metal catalysts.4 While efforts have yielded significant improvements with Fe- and Cometal catalysts,5,6 Ni remains challenging to rationally control and lower catalyst loadings.

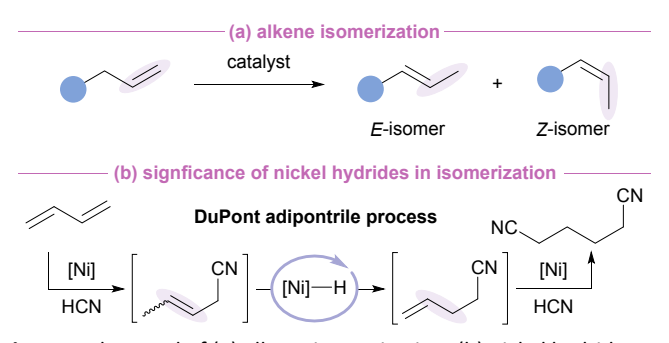


Fig. 1. Background of (a) alkene isomerisation, (b) nickel hydrides.

Notable advancements in Ni-H alkene isomerisation catalysts have been shown by Schoenebeck, Fleischer, Ogoshi, Koh, 10-12 Engle and Vantourout, 13 and Cook 14 which employ mild reaction conditions to achieve high yields and selectivities. However, a common drawback for these catalysts is the requirement of a strict inert atmospheric condition for reaction setup, significantly hindering synthetic practicality. Furthermore, these catalysts employ high Ni-metal loadings (10 mol %) or hazardous phosphine ligands, which hinder chemical sustainability. Lasty, a majority of these catalysts lack demonstration of tuneable ancillary ligands to achieve specific catalytic activity. Our group recently developed a modular Ni(0)/silane alkene isomerisation catalyst that is sterically tuneable through nitrogen-substitutes of N-heterocyclic carbene (NHC) ancillary ligands and electronically tuneable through 3° silanes; mechanistic experiments point towards a Ni-H active catalyst, which forms through the oxidative addition of a Si-H bond. 15 Despite these advances, this system has practical limitations, requiring strict airand moisture-free conditions and a multi-step synthetic process to obtain the Ni precatalyst. Additional drawbacks of this catalyst include lack of scalability (≤0.5 mmol) and a limited substrate scope consisting primarily of hydrocarbons. To overcome these limitations, we hypothesized that an analogous, second-generation catalyst catalyst could be formed in situ. Advantages for this design allows for rapid evaluation of reaction conditions to include air-tolerant species, commercially available or easily synthesized components, and the ability to finetune ancillary ligand properties for rationalising catalyst behaviour.

In this study, we report an *in situ*-generated alkene isomerisation catalyst using commercially available Ni(0) sources paired with an NHC ligand (the free carbene or the salt + base), and triphenylsilane. Through this approach, we rapidly evaluated a variety of NHCs with varied steric and electronic properties. The optimal NHC was found

ARTICLE Journal Name

to be MeIPr (1,3-bis(2,6-diisopropylphenyl)-4,5-dimethyl-2-imidazolylidene), achieving high product yield and *E*-selectivity. We show that this reaction readily proceeds at near-ambient temperature (30 °C) using MeIPr/Ni(COD)₂ (COD = 1,5-cyclooctadiene), albeit using the glovebox to set up the reaction to reach maximum efficiency. To circumvent glovebox usage, we developed a moisture-tolerant benchtop system using Ni(COD)(DQ) (DQ = duroquinone), an imidazolium salt, and base that efficiently isomerises alkenes at moderate reaction temperatures (60 °C). A diverse array of functional groups is tolerated. Preliminary mechanistic experiments including isotopic-labelling experiments and radical-probe studies suggest a Ni–H insertion/elimination pathway is occurring. This Ni(0)/silane catalyst offers increased modularity and synthetic practicality than previous reports, increasing its potential application in organic synthesis.

Results and discussion

Inspired by our previous work, in which (IPr)Ni(1,5hexadiene)/Ar₃SiH (IPr, 1,3-bis[2,6-bis(1-methylethyl)phenyl]-1,3dihydro-2*H*-imidazol-2-ylidene; Ar, aryl) was the optimal precatalyst, we hypothesized that the same active Ni-H catalyst could be generated in situ by reacting Ni(COD)2, IPr, and triphenylsilane (HSiPh₃). Under analogous reaction conditions (80 °C, toluene), allylbenzene (1a) was isomerised to β -methylstyrene (2a) in 87% yield and E/Z selectivity of 21:1 (Table 1, entry 1). Lowering the reaction temperature to 60 °C and 40 °C significantly diminished yields (46 and 20%, respectively, Table 1, entries 2-3), indicating that an elevated temperature is required with IPr, but increased the E/Z ratios. The thermodynamic E/Z ratio was reported to be 32.2:1 at 40 $^{\circ}$ C. 16,17 Using this data, we expect the following thermodynamic E/Zratios: 21.5:1 at 80 °C, 25.8:1 at 60 °C, and 35.6:1 at 30 °C (see ESI section 4c). The obtained E-selectivity values at 80 °C, 60 °C, and 40 °C with IPr (Table 1, entries 1-3) are consistent with these expected ratios.

Table 1. Optimization of the Ni(COD) $_2$ /NHC/Ph $_3$ SiH-catalysed alkene isomerisation. Yields and selectivity, reported as an average of two trials, determined by GC analysis using 1,2,4,5-tetramethylbenzene as an internal standard.

Entry	Deviation from standard conditions	Temp. (°C)	GC yield	Selectivity (E/Z)
1	=	80	87%	21:1
2	=	60	46%	26:1
3	-	40	20%	31:1
4	ITMe	40	5.0%	15:1
5	IMes	40	4.2%	13:1
6	SIPr	40	9.6%	31:1
7	^{CI} IPr	40	24%	43:1
8	Me IPr	40	86%	35:1
9	^{Me} lPr	30	81%	63:1

Taking advantage of the in situ catalyst design, we evaluated a series of NHCs with various steric and electronic parameters at 40 °C (Table 1, entries 4-8) to identify the optimal ligand. A set of readily accessible NHCs was evaluated and compared to IPr (Chart 1). ITMe (1,3,4,5-tetramethylimidazol-2-ylidene), **IMes** (1,3-bis[2,4,6trimethylphenyl]-1,3-dihydro-2H-imidazol-2-ylidene), and SIPr (1,3bis[2,6-diisopropylphenyl]-imidazolidine-2-ylidene) all gave lower yields of 2a (5.0%, 4.2%, and 9.6%; Table 1, entries 4-6, respectively) than IPr. However, using both ^{CI}IPr (1,3-bis[2,6-diisopropylphenyl]-4,5-dichloro-1,3-dihydro-2*H*-imidazol-2-ylidene) and MeIPr resulted in increased yields (24% and 86%; Table 1, entries 7 and 8, respectively) and selectivities (E/Z = 43:1 and 35:1, respectively), with MeIPr being identified as the best ligand in this series. Lowering the reaction temperature to 30 °C using MeIPr afforded a similar yield of 81% 2a with further increased E/Z selectivity to 63:1 (Table 1, entry 9), favouring the E-isomer. This E/Z ratio is larger than expected based on the calculated thermodynamic ratio (see discussion below on thermodynamic versus kinetic control of E/Z ratios).

To rationalize these trends, we compared the yields of 2a as a function of the ligand's percent buried volume ($%V_{Bur}$), a measure of the steric bulk of ligands.²¹ Compared to IPr ($%V_{Bur}$ = 36.9; 20% yield 2a; 31:1 E/Z), using smaller ligands such as ITMe ($%V_{Bur}$ = 26.1) and IMes ($%V_{Bur}$ = 33.7) resulted in lower yields of 2a (5.0% and 4.2%, respectively) and worse E/Z selectivity (15:1 and 13:1, respectively).^{18,21} CIPr ($%V_{Bur}$ = 39.1) and MeIPr ($%V_{Bur}$ = 39.6) are

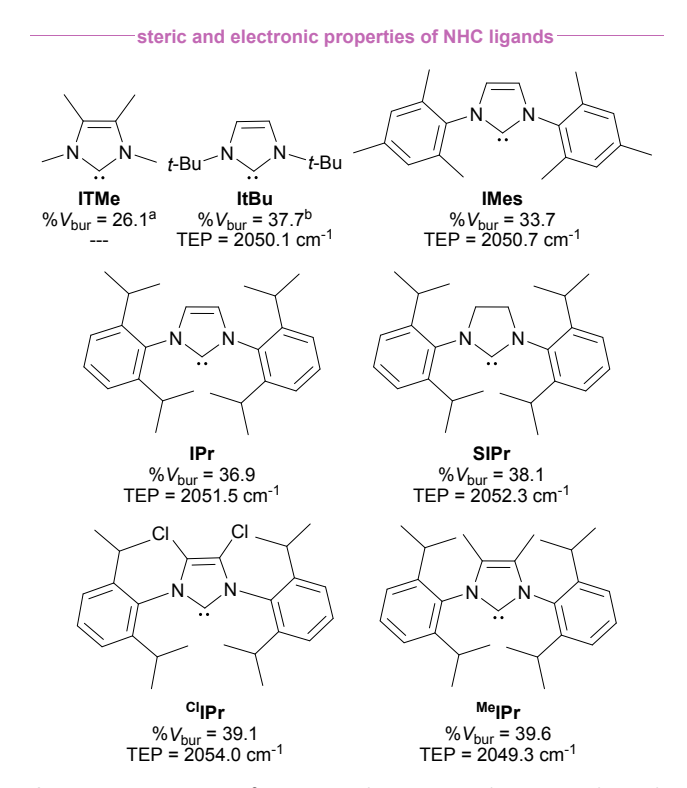


Chart 1. Structures of NHCs with associated percent buried volumes (top, $%V_{Bur}$) and Tolman electronic parameters (bottom, TEP, cm⁻¹) from present literature. $%V_{Bur}$ calculated with Ni–C_{carbene} at 2.00 Å from [(NHC)Ni(styrene)₂] complexes.¹⁶ TEPs reported from [IrCl(NHC)(CO)₂] complexes measured in DCM.^{18–22} a % V_{Bur} reported from [(ITMe)AuCl] complex. b % V_{Bur} reported from [(itBu)Ni(allyl)Cl] complex.

Journal Name ARTICLE

Table 2. Reaction optimization using Ni(COD)(DQ), an imidazolium salt, and a base for the isomerisation of **1b**. Yields and selectivity, reported as an average of two trials, determined by GC analysis using cyclooctane as an internal standard. ^an.d., not determined. ^breported at 1 h.

Entry	Deviation from standard conditions	GC yield	Selectivity (E/Z)
1	none	94%	24:1
2	Ambient air	0%	n.d. ^a
3	No Ni(COD)(DQ)	0%	n.d.
4	No KO <i>t</i> -Bu	0%	n.d.
5	No HSiPh₃	8%	74:1
6	No IPr∙HBF ₄	0%	n.d.
7	IPr∙OTf	92%	23:1
8	ItBu∙HBF₄	0%	n.d.
9	IMes•HBF ₄	11%	32:1
10	^{Me} IPr∙HBF ₄	97%	25:1
11	MeIPr•HBF _{4,} 50 °C	0% ^b	n.d.

sterically larger than IPr, and they give higher yields of 2a (24% and 86%, respectively) and better E/Z selectivity (43:1 and 35:1, respectively). One outlier in this trend is with SIPr (% V_{Bur} = 38.1) which yielded only 9.6% of 2a despite being sterically larger than IPr.²¹ We attribute this decreased reactivity to the saturated backbone which increases the torsion angle of the N-C_{carbene}-N angle of the NHC ligand.²¹ To further explain the differences between the unsaturated series (IPr, CIPr, and MeIPr) we explored electronic effects measured by Tolman Electronic Parameter values (TEPs). CIPr (TEP = 2054.0 cm⁻¹) is less σ -donating than IPr (TEP = 2051.5 cm⁻¹), and has a slightly higher yield of $2a.^{22~\text{Me}IPr}$ is more $\sigma\text{-donating}$ than IPr (TEP = 2049.3 cm^{-1} and 2051.5 cm^{-1} , respectively) and gives the highest yield of 2a.22 Therefore, the trends in yield and selectivity as a function of ligand correlate more strongly with the steric bulk of the ligand, as measured by $%V_{Bur}$, than the electronics of the ligand, as measured by TEP values.

After establishing the in situ alkene isomerisation catalytic system using Ni(COD)2, we sought to developed a more practical reaction setup that uses air-tolerant reagents. We exchanged the airsensitive Ni(COD)₂ for air-stable Ni(COD)(DQ) and the free NHC to an imidazolium salt with a base to form the free carbene in solution.²³ Testing the isomerisation of 4-allylanisole (1b) using IPr•HBF4 and KOt-Bu at 60 °C afforded 94% 2b with a selectivity of 24:1 (E/Z) after 6 h (Table 2, entry 1). Notably, all reactions were setup on the benchtop, and the results in Table 2, except for entry 2, were collected using nitrogen-sparged solvent and flushing the reaction vessel with nitrogen gas; however, no reactivity is observed when the reaction is run under ambient air (Table 2, entry 2). These data suggest that water does not impact catalysis, but oxygen does inhibit the desired activity. Control experiments demonstrated the necessity of each reaction component for isomerisation, as very little (or no) 2b is formed upon the exclusion of the Ni source, imidazolium

salt, base, or silane (Table 2, entries 3-6). We next investigated the characteristics of the imidazolium salt. Exchanging the BF₄ counter ion with triflate (OTf) yielded similar results (92% yield, E/Z = 23:1, Table 2, entry 7). Replacing IPr•HBF₄ with a less flexible, yet sterically demanding imidazolium salt, ItBu•HBF₄ (1,3-di-tertbutylimidazolium tetrafluoroborate), yielded no catalytic activity (Chart 1 and Table 2, entry 8). Utilising sterically smaller imidazolium salt, IMes•HBF4, resulted in minimal isomerisation (Table 2, entry 9). 18 However, increasing the steric bulk with the addition of MeIPr, as seen in the Ni(COD)₂/NHC system, improved the yield to 97% while maintaining similar selectivity (E/Z = 25:1) (Table 2, entry 10). We attempted to lower the reaction temperature from 60 °C to increase E-selectivity, however isomerisation no longer occurred, which we attribute to low solubility of the precatalyst and additives (Table 2, entry 11).

Because the yield and selectivity of 2b with IPr•HBF4 and MeIPr•HBF₄ are similar at 6 h reaction time (Table 2, entries 1 and 10), we sought to differentiate their activity by monitoring the isomerisation of 1b to 2b over time (Fig. 2). While the maximum yield is reached within 25 min with MeIProHBF4 (Fig. 2, purple circles), completion is not reached within 3 hours using IPr•HBF4 (Fig. 2, pink squares). Furthermore, IPr•HBF4 shows a significant induction period (~45 min), while MeIPr•HBF₄ shows a negligible, if any, induction period. When MeIProHBF4 is used, the E/Z selectivity of 2b starts at 34:1, and equilibration continues for ~125 min, reaching a final selectivity of 23:1 (see ESI section 4d Fig. S2). Because the E/Z ratio at the beginning of the reaction is higher than the calculated thermodynamic ratio, we believe that the reaction is under kinetic control at the beginning of the reaction, and as the reaction time progresses, thermodynamic factors dominate, and the E/Z ratio decreases. Because of the faster initial rate, MeIPr•HBF₄ was chosen as the optimal NHC precursor for isomerisation.

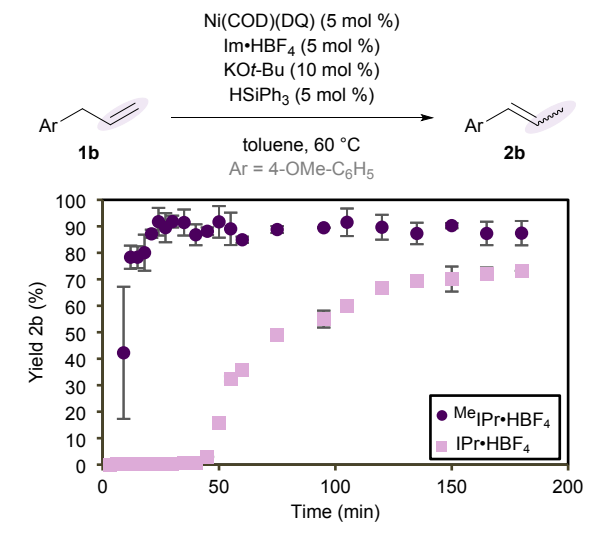


Fig. 2. Yield of **2b** measured over time using MeIPr•HBF₄ (purple circles) and IPr•HBF₄ (pink squares) as NHC precursors. Yields and selectivity reported as an average of two trials, determined by GC analysis using cyclooctane as an internal standard.

Moving forward with optimized conditions, we tested a variety of alkene substrates (Fig. 3). The electron-poor allylbenzene

ARTICLE Journal Name

Fig. 3. Substrate scope of alkene isomerisation (p.s., positional selectivity).

derivative, 4-CF₃-allylbenzene (1c) yields 76% product (2c) with 33:1 selectivity. The acid-sensitive methoxymethyl ether group was welltolerated, with product 2d forming in high reaction yield (97%) with 20:1 selectivity (E/Z). 4-Br-allylbenzene (1e) affords 53% yield of 2e with 14:1 selectivity (E/Z); this tolerance of an aryl bromide is notable, since Ni complexes are known to react readily with them in oxidative addition reactions.²⁴ Trisubstituted alkenes are formed in high yields and moderate selectivity, as shown with 2-phenyl-2pentene (2f) (94% yield, E/Z = 11:1). Added steric bulk, as seen in 2methylallylbenzene (1g) and allylmesitylene (1h), resulted in moderate to good yields but with a decrease in selectivity (E/Z = 10:1and 2.0:1, respectively). Alkene isomerisation can be achieved across multiple bonds, as demonstrated with 1-decene (1i) and homoallylbenzene (1j) to afford a mixture of positional isomers (positional selectivity, p.s. = 1:2.1 and 2.3:1, respectively), and the major isomer of **2j** being 1-buten-1-ylbenzene (E/Z = 34:1). The catalyst system tolerates a variety of aromatic heterocycles including pyridine (1k), indole (1l), thiophene (1m), furan (1n), affording 2k, 2l, 2m, and 2n, respectively, in good conversions or yields (84-98%) and moderate to good selectivity (E/Z = 4.5-18:1). Notably, this tolerance of heterocycles is a drastic improvement compared to our previously reported (IPr)Ni(1,5-hexadiene) catalyst. 15 Other functional groups such as a tertiary amine to form an enamine (20) and a β , γ unsaturated amide to form an α,β -unsaturated amide (2p) are suitable for this reaction, which are also further improvements over previous work. To demonstrate the value and usefulness of this system, a large-scale reaction with 1b was performed and 1.17 g 2b (98% yield) was isolated in good selectivity of E/Z = 25:1, with the entire reaction set up on the bench with sparging. To exemplify the synthetic utility of enamines generated with our catalyst, a tandem reaction was performed converting allyldiphenylamine (10) to 20, and then adding benzaldehyde, resulting in the formation of 2methyl-3-phenyl-2-propen-1-al (3a) in 63% yield.

We next performed mechanistic experiments to extract information on the reaction pathway. We considered three common pathways for Ni-catalysed alkene isomerisation including (i) a radical pathway through metal-hydride atom transfer (MHAT), (ii) an

intramolecular π -allyl pathway, and (iii) a metal-hydride (M–H) insertion/elimination pathway (Fig. 4a). To differentiate between these possibilities, we performed experiments to unveil the reaction mechanism. We hypothesized that, once the active catalyst is formed, the mechanism would be analogous to our previously reported catalyst's mechanism, for which evidence supports an insertion/elimination pathway, ¹⁵ so we performed a similar set of experiments to identify any differences. Notably, these experiments were also chosen because they would provide evidence against at least one of the three pathways considered.

As shown in Table 2, HSiPh₃ is necessary for catalytic activity; we hypothesized that it acts as a hydride source to form the Ni-H active catalyst. Using our standard conditions, the isomerisation of 1b to 2b was performed using DSiPh₃ to determine if the hydrogen from the silane is incorporated into the product. Deuterium incorporation into the propenyl group is expected for insertion/elimination and MHAT pathways, while no deuterium incorporation is expected for the π allyl pathway, since the M-H in the π -allyl pathway is formed via C-H activation of an allylic C-H bond. Using substrate 1b, ²H NMR shows D-incorporation in all three positions along the propenyl chain of 2b (Fig. 4b, top), indicating that isomerisation is likely occurring via an MHAT or insertion/elimination pathway. Additionally, the presence of deuterium at all three positions of the propenyl group demonstrate that isomerisation is highly reversible. To further understand catalyst behaviour, an additional experiment using DSiPh₃ was performed using α-propylstyrene (**1f**) as the substrate. Dincorporation was only observed in the β-methyl group of 2f (Fig. 4b, bottom), signifying that isomerisation is irreversible for trisubstituted alkenes. This change in reactivity between trisubstituted and 1,2-disubstituted alkenes supports the feasibility of the insertion/elimination pathway, since it is known that trisubstituted alkenes are worse ligands for Ni than 1,2-disubstituted alkenes, and they readily dissociate before migratory insertion can occur.25 Additionally, these D-incorporation studies support our hypothesis that the silane acts as the hydride source and are consistent with the MHAT and insertion/elimination pathways but inconsistent with the π -allyl pathway.

A crossover experiment was performed to differentiate between an intra- $(\pi\text{-allyl})$ and intermolecular (MHAT or Ni–H

Journal Name ARTICLE

insertion/elimination) mechanism. A 1:1 mixture of α -propylstyrene (1f) and 4'-OMe- α -ethylstyrene- d_2 (1q- d_2) were subjected to the standard reaction conditions (Fig. 4c). If the reaction proceeds through an intramolecular pathway, no deuterium incorporation into 2f is expected, while if an intermolecular pathway is operative, deuterium incorporation would be expected in 2f. 2 H NMR analysis displays deuterium incorporation into both products 2f and 2q, which is consistent with the intermolecular pathways, and is inconsistent with the π -allyl pathway.

For our final mechanistic endeavour, we probed the reaction for an MHAT pathway by subjecting a 1,6-diene radical clock (1r) to the standard isomerisation conditions (Fig. 4d). If the reaction proceeds through an MHAT pathway, a free radical intermediate will be generated, and 1r will cyclize into a cyclopentane ring. However, if

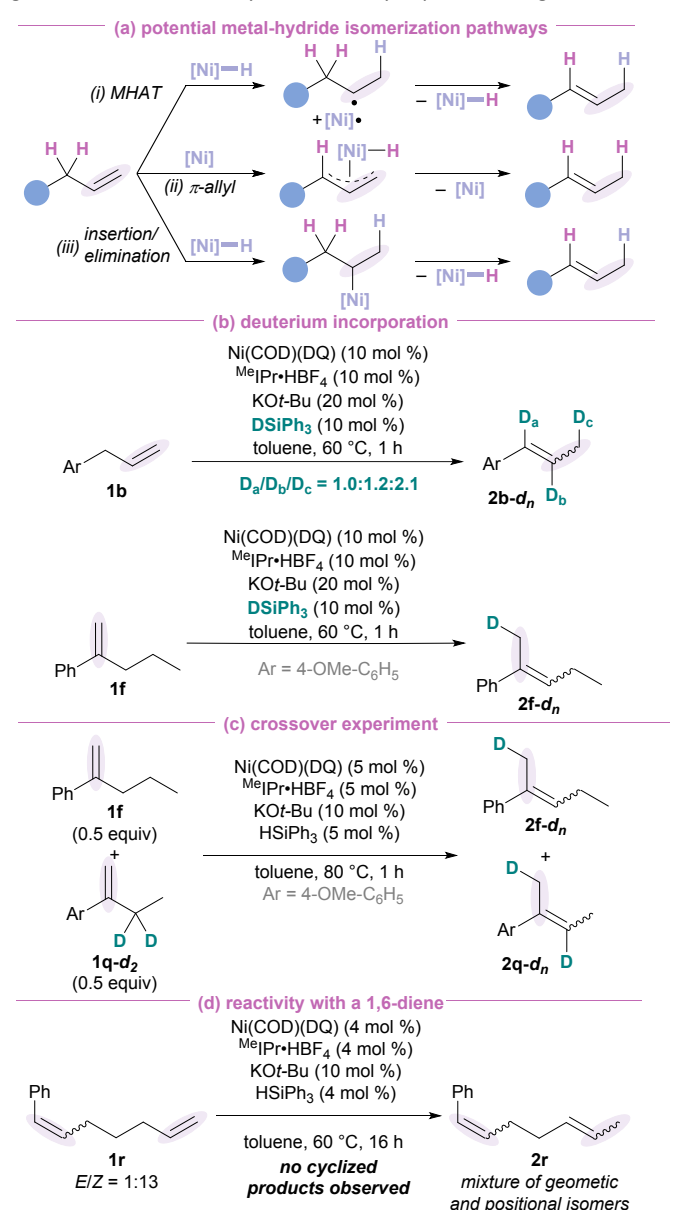


Fig. 4. (a) Potential metal-hydride pathways. (b) Deuterium incorporation experiment. (c) Deuterium crossover study. (d) Radical probe experiment with 1,6-diene.

the reaction proceeds through a two-electron pathway (Ni–H insertion/elimination or π -allyl) no cyclized products are expected to form. Reacting 1r under standard conditions, only geometric and positional isomerisation products were observed, and no cyclized products were detected as determined by ^1H NMR analysis. This result suggests that radical species are likely not generated in our catalytic system.

Collectively, these experiments support a Ni–H insertion/elimination mechanism. The Ni–H can be accessed through oxidative insertion of Ni into the R₃Si–H bond; migratory insertion of the coordinated alkene into the Ni–H bond followed by β -hydride elimination to generate the product. Ligand exchange of the isomerised alkene for the starting alkene completes the catalytic cycle.

Conclusions

In conclusion, we have developed a practical alkene isomerisation protocol using Ni(0), a silane, and an NHC ancillary ligand. The NHC can be readily modulated to induce desirable catalytic activity. Enabled by the avoidance of the cumbersome and challenging synthesis of (NHC)Ni(0) complexes, MeIPr was rapidly identified as the best ligand. Under optimized conditions, high yields and *E/Z* selectivities are obtained for a variety of substrates, including allylbenzene derivatives, heterocycles, 1,1-disubstituted alkenes, and enamines. Mechanistic studies suggest the alkene isomerisation pathway proceeds through a Ni–H insertion/elimination route. This bench-preparative catalytic system serves as an attractive synthetic method to form internal alkenes from readily abundant terminal alkenes, with facile ligand modularity.

Conflicts of interest

There are no conflicts to declare.

Data availability

The data supporting this article have been included as part of the Supplementary Information.†

Acknowledgements

This research was supported by the Office of the Vice President of Research and the College of Arts and Sciences at the University of Oregon. M.A.K. acknowledges the ARCS Foundation Oregon ARCS for a fellowship. A.S.C. acknowledges the NSF for a GRFP fellowship.

Notes and references

 C. R. Larsen and D. B. Grotjahn, in Applied Homogeneous Catalysis with Organometallic Compounds, John Wiley & Sons, Ltd, 2017, pp. 1365–1378. ARTICLE Journal Name

- J. J. Molloy, T. Morack and R. Gilmour, Angew. Chem. Int. Ed., 2019, 58, 13654–13664.
- 3. E. Larionov, H. Li and C. Mazet, *Chem. Commun.*, 2014, **50**, 9816–9826.
- 4. X. Liu, B. Li and Q. Liu, Synthesis, 2019, **51**, 1293–1310.
- X. Yu, H. Zhao, P. Li and M. J. Koh, J. Am. Chem. Soc., 2020, 142, 18223–18230.
- S. Zhang, D. Bedi, L. Cheng, D. K. Unruh, G. Li and M. Findlater, J. Am. Chem. Soc., 2020, 142, 8910–8917.
- A. Kapat, T. Sperger, S. Guven and F. Schoenebeck, *Science*, 2019, 363, 391–396.
- P. M. Kathe, A. Caciuleanu, A. Berkefeld and I. Fleischer, J. Org. Chem., 2020, 85, 15183–15196.
- H. Iwamoto, T. Tsuruta and S. Ogoshi, ACS Catal., 2021, 11, 6741–6749.
- C.-F. Liu, H. Wang, R. T. Martin, H. Zhao, O. Gutierrez and M. J. Koh, *Nat. Catal.*, 2021, 4, 674–683.
- 11. L. Huang, E. Q. Lim and M. J. Koh, *Chem Catal.*, 2022, **2**, 508–518.
- 12. Y. Zhao, C.-F. Liu, L. Q. H. Lin, A. S. C. Chan and M. J. Koh, *Angew. Chem. Int. Ed.*, 2022, **61**, e202202674.
- 13 C. Z. Rubel, A. K. Ravn, H. C. Ho, S. Yang, Z.-Q. Li, K. M. Engle and J. C. Vantourout, *Angew. Chem. Int. Ed.*, 2024, **63**, e202320081.
- A. S. Chang, M. A. Kascoutas, Q. P. Valentine, K. I. How, R. M. Thomas and A. K. Cook, *J. Am. Chem. Soc.*, 2024, **146**, 15596– 15608.
- K. E. Kawamura, A. S. Chang, D. J. Martin, H. M. Smith, P. T. Morris and A. K. Cook, *Organometallics*, 2022, 41, 486–496.
- 16. E. Taskinen and N. Lindholm, *J. Phys. Org. Chem.*, 1994, **7**, 256–258.
- 17. A. Bansal and S. D. Jackson, *React. Kinet. Mech. Catal.*, 2022, 135, 1457–1468.
- 18. H. Clavier and S. P. Nolan, Chem. Commun., 2010, 46, 841–861.
- 19. R. A. Kelly III, H. Clavier, S. Giudice, N. M. Scott, E. D. Stevens, J. Bordner, I. Samardjiev, C. D. Hoff, L. Cavallo and S. P. Nolan, *Organometallics*, 2008, **27**, 202–210.
- T. Dröge and F. Glorius, Angew. Chem. Int. Ed., 2010, 49, 6940–6952.
- S. Felten, S. F. Marshall, A. J. Groom, R. T. Vanderlinden, R. M. Stolley and J. Louie, *Organometallics*, 2018, 37, 3687–3697.
- 22. M. Pompeo, R. D. J. Froese, N. Hadei and M. G. Organ, *Angew. Chem. Int. Ed.*, 2012, **51**, 11354–11357.
- V. T. Tran, Z.-Q. Li, O. Apolinar, J. Derosa, M. V. Joannou, S. R. Wisniewski, M. D. Eastgate and K. M. Engle, *Angew. Chem. Int. Ed.*, 2020, 59, 7409–7413.
- 24. T. T. Tsou and J. K. Kochi, *J. Am. Chem. Soc.*, 1979, **101**, 6319–
- 25. C. A. Tolman, J. Am. Chem. Soc., 1974, 96, 2780-2789.

Footnote

† Electronic supplementary information (ESI) available. See DOI: 10.1039/x0xx00000x

The data supporting this article have been included as part of the Electronic Supplementary Information.